



THE UNIVERSITY *of* EDINBURGH

Edinburgh Research Explorer

## Effect of Radius Ratio on Natural Convection Heat Transfer inside an Eccentric Semicircular Enclosure

**Citation for published version:**

Das, PK & Mahmud, S 2000, Effect of Radius Ratio on Natural Convection Heat Transfer inside an Eccentric Semicircular Enclosure. in *Sixth Annual Paper Meet and International Conference.*, Paper No. 7, pp. 46–53.

**Link:**

[Link to publication record in Edinburgh Research Explorer](#)

**Document Version:**

Publisher's PDF, also known as Version of record

**Published In:**

Sixth Annual Paper Meet and International Conference

**General rights**

Copyright for the publications made accessible via the Edinburgh Research Explorer is retained by the author(s) and / or other copyright owners and it is a condition of accessing these publications that users recognise and abide by the legal requirements associated with these rights.

**Take down policy**

The University of Edinburgh has made every reasonable effort to ensure that Edinburgh Research Explorer content complies with UK legislation. If you believe that the public display of this file breaches copyright please contact [openaccess@ed.ac.uk](mailto:openaccess@ed.ac.uk) providing details, and we will remove access to the work immediately and investigate your claim.



**EFFECT OF RADIUS RATIO ON NATURAL CONVECTION HEAT  
TRANSFER INSIDE AN ECCENTRIC SEMICIRCULAR ENCLOSURE**

P. K. Das and S. Mahmud

Department of Mechanical Engineering, Bangladesh University of Engineering &  
Technology, BUET, Dhaka-1000

**ABSTRACT**

This paper presents the effect of radius ratio on natural convection heat transfer and fluid flow inside an eccentric semicircular enclosure with isothermal upper and lower surface. Here laminar steady natural convection heat transfer inside the eccentric enclosure were observed for radius ratio  $R^* = 1.75, 2.0, 2.25, 2.5$  keeping eccentricity ( $\epsilon=0.4$ ) constant. The differential forms of governing equations are solved by using Finite-Difference method. Simulation was carried out for ranges of Grashof number  $10^1$  to  $10^7$ . Results are presented in the form of constant streamfunction, isothermal lines, local Nusselt number and average Nusselt number at different angular position. Radius ratio has significant effect on natural convection heat transfer as well as on flow field.

**1. INTRODUCTION**

Natural convection heat transfer inside annular space, air-filled cavity or annular sector has wide application in many engineering problems. In our earlier work [1], we have shown the effect of eccentricity on heat transfer and flow field for radius ratio  $R^*=2.0$  for different eccentricity ( $\epsilon=0.2, 0.4, 0.6$ ). Kuhen & Goldstein [4-6] presented reviews of the available literature and experimental results in concentric and eccentric horizontal cylindrical annuli. Glakpe et. al. [7] examined effect of mixed boundary condition on heat transfer in eccentric enclosures. Yang et. al. [8] investigated steady laminar natural convection in a maximum eccentric ( $\epsilon=1.0$ ) horizontal annulus with different diameter ratios and three eccentric position. Some other numerical works are presented [9-10] heat transfer inside eccentric cylindrical annuli. In this paper, laminar steady natural convection heat transfer inside an eccentric enclosure bounded by two semicircular surface of different diameter is studied at eccentricity of 0.4 with four different radius ratio. Rate of heat transfer in terms of local and global Nusselt numbers are presented for different angular positions of inner semicircular surface and Grashof number respectively. Flow and thermal fields are analyzed by parametric presentation of streamlines and isothermal lines.

## 2. PROBLEM FORMULATION

Consider a fluid enclosed in a space bounded by two semicircular surface of radius  $R_o$  and  $R_i$  as shown in Fig.1. The surface of the semicircular surface are maintained at constant uniform temperatures  $T_i$  and  $T_o$ , where  $T_i > T_o$ . Two horizontal surfaces that connect outer and inner semicircular surface are considered adiabatic. Assuming that the Boussinesq approximation is valid, the dimensionless equations governing the two-dimensional fluid motion may be reduced to:

$$\text{div } \mathbf{V} = 0 \quad (1)$$

$$(\mathbf{V} \cdot \mathbf{grad})U = -\frac{\partial p}{\partial r} + Ra Pr T \cos \theta + Pr \rho_r \mathbf{V} \quad (2)$$

$$(\mathbf{V} \cdot \mathbf{grad})V = -\frac{\partial p}{r \partial \theta} + Ra Pr T \sin \theta + Pr \rho_r \mathbf{V} \quad (3)$$

$$(\mathbf{V} \cdot \mathbf{grad})T = \rho_r T \quad (4)$$

$$\rho_r = \rho_{ref} [1 - \beta (T - T_{ref})] \quad (5)$$

Where  $\rho_{ref}$  is the density of the fluid at some reference temperature  $T_{ref}$  and  $\beta$  is the coefficient of thermal expansion. Schematic diagram of the problem under consideration

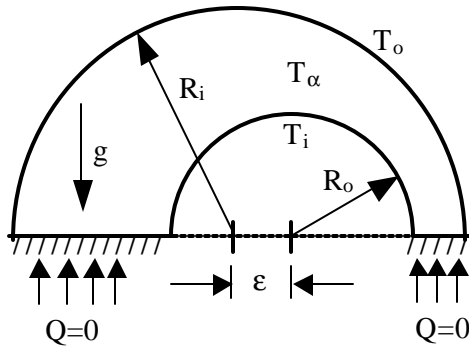


**Fig.1: Schematic diagram of problem under consideration**

is shown in Fig.1 with various geometrical parameters where radius ratio is defined as ratio between the outer radius and inner radius. The total solution domain is divided into finite number of control volume. Governing equations are then solved using control-volume-based Finite Difference method described by Chai & Patankar [2] and Patankar [3].

## 3. RESULTS AND DISCUSSIONS

Three grid sizes (30\*16, 60\*32, and 120\*64) were chosen to carry out present simulation. Results are presented for fine grid (120\*64). For a particular eccentricity, Grashof number was varied by changing dynamic viscosity keeping other fluid and geometric variables constant. Iteration was stopped when

difference between two consecutive variable values for all variables fall below  $10^{-5}$ . For further stabilization of numerical procedure, under relaxation factor was chosen between 0.1-0.7.

### 3.1 Local heat transfer

Local Nusselt number distribution along the surface of lower semicircular surface is shown in Fig.2 for  $Gr=10^2, 10^5$ . At  $Gr=10^2$ , heat transfer is almost invariant

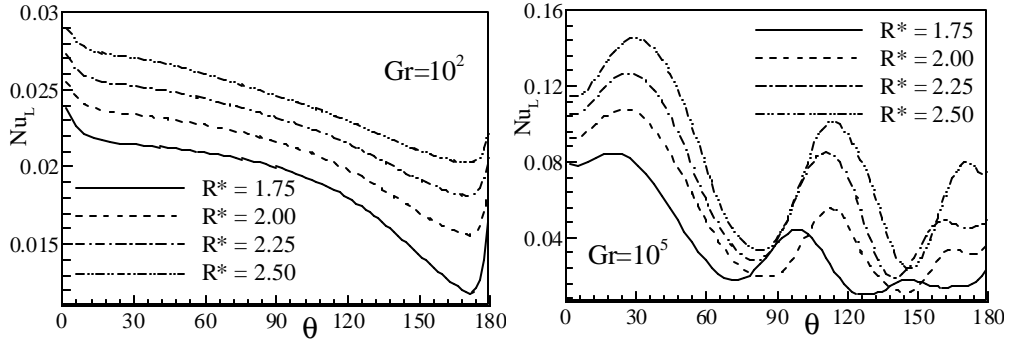


**Fig.2: Variation of local Nusselt number along lower semicircular surface,  $q$  is measured from left to right (clockwise) over the lower semicircle**

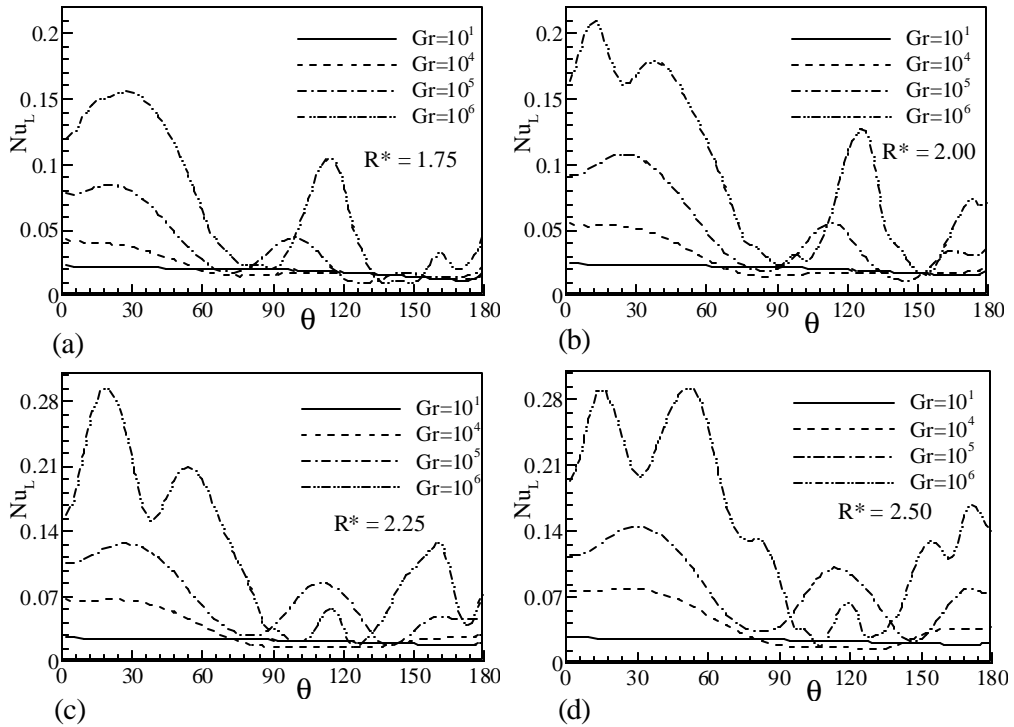


**Fig.3: Local Nusselt number distribution at fixed  $R^*$  and different  $Gr$**

along the periphery of the lower semicircular surface except two corners for  $\epsilon=0.0$ . But At  $\epsilon=0.4$ , heat transfer rate is higher than concentric case for angular position ( $\theta$ ) between  $0^\circ$  to  $100^\circ$ . Between  $100^\circ$  to  $180^\circ$  heat transfer rate is lower. For each radius ratio, same heat transfer pattern is observed having higher rate of heat transfer at higher  $R^*$ . Interesting scenario is observed at  $Gr=10^5$  and periodic heat transfer rate (with respect to angular position) is observe for different radius ratio. This is happened due to symmetric multicellular flow inside the enclosure. For lower radius ratio, symmetrical nature of multicellular flow corrupts causing breakdown the periodic nature of heat transfer. This is shown in Fig.2 (b). Fig.3 shows the Nusselt number distribution at different Grashof number for constant radius ratio.

### 3.2 Average heat transfer

The effect of radius ratio on average heat transfer in an eccentric enclosure is shown in the Fig. 4. At lower Grashof number the effect of radius ratio is very small but at higher Grashof number the effect is significant. At higher radius ratio heat transfer rate is higher than the lower one.

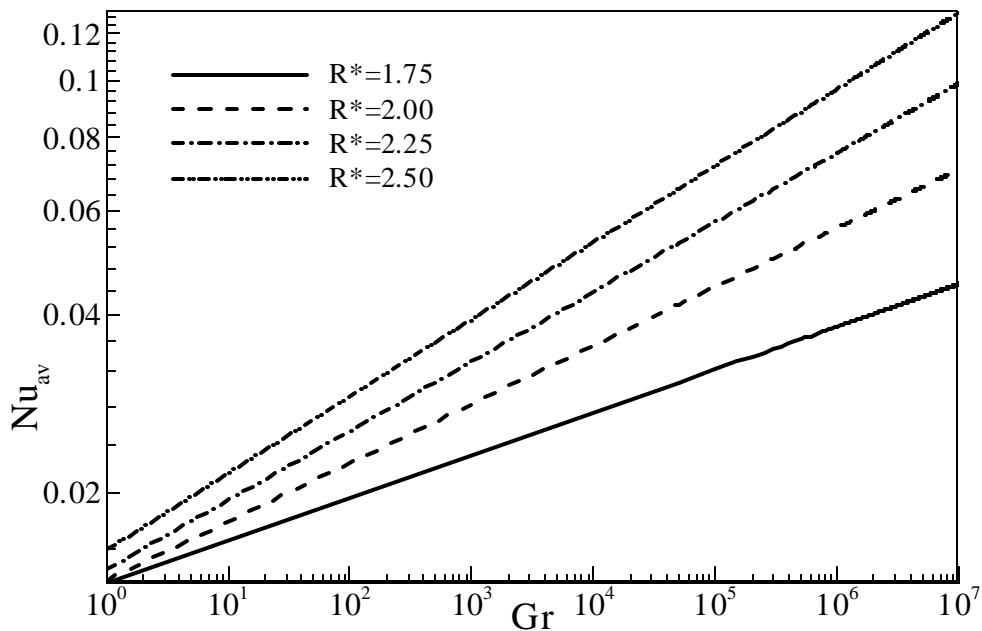


**Fig.4: Variation of average Nusselt number with Grashof numbers for different radius ratio**

### 3.3 Flow field

Fig.5 shows the constant streamfunction contours at six different Grashof number for  $R^*=2.5$ . At  $Gr=10^1$ , bicellular flow is observed with one crescent-shape vortex at narrower cross section. Bicellular flow turns into tricellular in between  $Gr=10^4 - 2*10^4$ . At  $Gr=5*10^4$ , multicellular flow with three small vortex at narrower cross

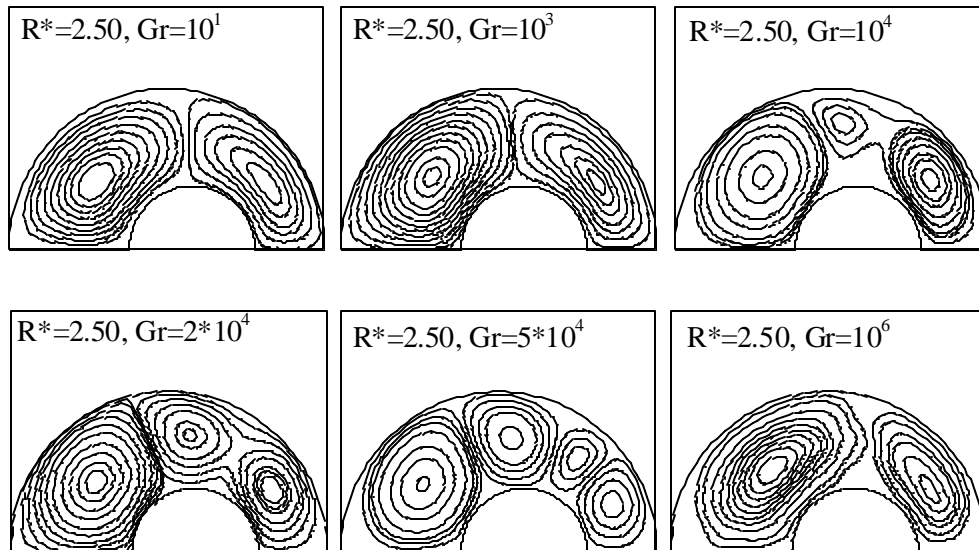
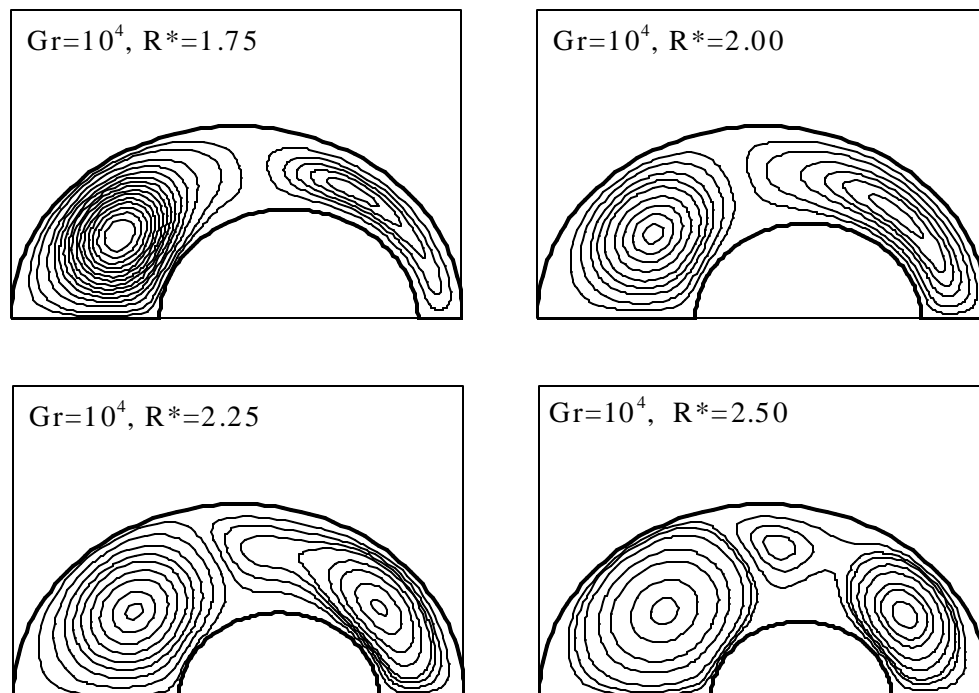


**Fig.5: Streamlines at different Grashof number for  $R^*=2.5$**



section and one large vortex at larger cross section is observed. Instability in hydrodynamic boundary layer at narrower cross section breaks the crescent-shape vortex into three separate small circular zones. The distorted streamlines at  $Gr=10^6$  indicate transition to turbulence but interesting pattern is observed here that the multicellular pattern is dissolved into bicellular pattern again. Fig.6 shows the effect of radius ratio on flow field at constant Grashof number  $10^4$ . Higher radius ratio shifts the core of crescent-shape vortex of narrower cross section downward shown in the Fig. 6(a) and Fig. 6(b). But at radius ratio  $R^*=2.25$  crescent-shape vortex break down into two cell and at  $R^*=2.5$  we observed tricellular pattern whereas at lower radius ratio bi-cellular pattern is found. The vortex of larger cross section remains unchanged with the increase of radius ratio.

### 3.3 Thermal field

Isothermal lines in Fig.7 present the thermal field for  $R^*=2.5$ . At  $Gr=10$ , buoyancy effect is almost negligible. Isothermal lines are semicircular in shape showing uniform temperature gradient normal to the lower semicircular surface. Isothermal lines concentrated near the left most corner of the inner semicircular surface showing higher temperature gradient. Other parts of the enclosure show uniform distribution of isothermal lines. Transition to tricellular flow changes the isotherm pattern at  $Gr=10^4$ . Clear three spots of high nearwall temperature gradient normal to the inner semicircular surface is observed at  $Gr=2*10^4$  (Fig.7d). Heat transfer rates higher at these spots. Similar pattern is observed at  $Gr=5*10^4$  but temperature gradient is higher than previous case and the hot plume of the temperature pattern is developed fully here and a portion of isotherms becomes swirl shown in Fig.7 (e). This is due to present of multicellular flow pattern. The distorted isothermal lines at  $Gr=10^6$  indicate transition to turbulence.

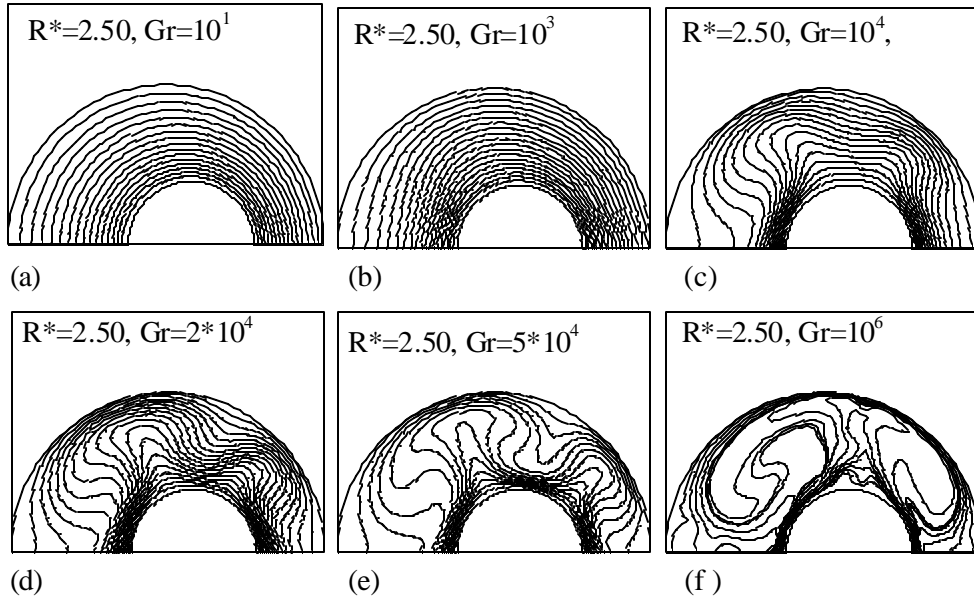


**Fig.7: Isothermal lines at different Grashof numbers for  $R^* = 2.5$**

#### 4. CONCLUSIONS

Effect of radius ratio on natural convection heat transfer and buoyancy-induced flow inside a semicircular eccentric enclosure is investigated numerically. Radius ratio affects both local heat transfer pattern and flow field. Introducing eccentricity changes the true periodic pattern of local heat transfer of concentric enclosure. But radius ratio has significant influence on average heat transfer rate. Crescent-shape vortex is observed at smaller cross sectional area at lower Grashof number, which distorted into bicellular and then into multicellular pattern at higher Grashof number. But the vortex of larger cross sectional area remains almost unchanged with the increase of Grashof number. At Grashof number  $10^4$  multicellular vortex is found at higher radius ratio which indicate that with increase of radius ratio critical Grashof number decreases.

#### NOMENCLATURE

$g$	= gravity vector	$T_0$	= outer wall temperature
$Gr$	= Grashof number, $(\rho^2 g \beta \Delta T R_o / \mu^2)$	$T_\alpha$	= fluid temperature
$h$	= convective heat transfer coeff.	$T_{ref}$	= reference temperature
$K_f$	= thermal conductivity of fluid	$Q$	= heat transfer rated
$Nu_L$	= local Nusselt number, $(h R_o / K_f)$	<i>Greek symbol</i>	
$Nu_{av}$	= average Nusselt number	$\beta$	= thermal expansion coeff.
$p$	= pressure	$\varepsilon$	= eccentricity
$R_i$	= radius of inner semicircle	$\mu$	= dynamic viscosity
$R_o$	= radius of outer semicircle	$\rho$	= mass density
$R^*$	= radius ratio	$\theta$	= angular position
$T_i$	= inner wall temperature	$\Delta_{r,\theta}$	= Laplacian symbol

#### REFERENCE

- [1] P. K. Das, S. Mahmud, Buoyancy induced flow and heat transfer inside a semicircular eccentric enclosure, Proc. of 3<sup>rd</sup> ICFMHT'99, p.p.270-275, 1999
- [2] J. C. Chai, S. V. Patankar, Laminar natural convection in internally finned horizontal annuli, Numerical Heat Transfer, vol.24, 1993
- [3] S. V. Patankar, Numerical heat transfer and fluid flow, McGraw-Hill, New York, 1980
- [4] T. H. Kuhen, R. J. Goldstein, An experimental and theoretical study of natural convection in the annulus between horizontal concentric cylinders, J. Fluid Mech. vol. 74, 1976
- [5] T. H. Kuhen, R. J. Goldstein, An experimental study of natural convection heat transfer in concentric and eccentric horizontal cylindrical annuli, J. Heat Transfer, vol. 100, 1978



- [6] T. H. Kuhen, R. J. Goldstein, A parametric study of Prandtl number and diameter ratio effects on natural convection heat transfer in horizontal cylindrical annulus, *J. Heat Transfer*, vol. 102, 1980
- [7] E. K. Glakpe, C. B. Watkins, Effect of mixed boundary conditions on natural convection in concentric and eccentric annular enclosure, *AIAA Paper*, 1987
- [8] Z. Yang, J. He, A study of natural convection heat transfer in a maximum eccentric horizontal annulus, *Proc. of 11<sup>th</sup> IHTC*, vol. 3, 1998
- [9] C. H. Cho, K. S. Chang, K. H. Park, Numerical simulation of natural convection in concentric and eccentric horizontal annuli, *ASME, J. of Heat Transfer*, vol. 104, 1982
- [10] J. Prusa, L. S. Yao, Natural convection heat transfer between eccentric horizontal cylinders, *ASME, J. of Heat Transfer*, vol. 105, 1983